

Specific features in the synthesis, crystal structure and electrical conductivity of BICUTIVOX

M.V. Morozova ^{a,*}, E.S. Buyanova ^a, Yu.V. Emelyanova ^a, V.M. Zhukovskiy ^a, S.A. Petrova ^b, R.G. Zakharov ^b, N.V. Tarakina ^c

^a Department of Chemistry, Ural State University, 51 Lenin Ave., 620083, Ekaterinburg, Russia

^b Institute for Metallurgy, Ural Branch of the Russian Academy of Sciences, 101 Amundsen Str., 620016, Ekaterinburg, Russia

^c Institute of Solid State Chemistry, Ural Branch of the Russian Academy of Sciences, 91 Pervomayskaya Str., 620990, Ekaterinburg, Russia

ARTICLE INFO

Article history:

Received 20 January 2011

Received in revised form 14 June 2011

Accepted 15 July 2011

Available online 22 September 2011

Keywords:

BIMEVOX

Oxygen-ion conductors

Crystal structure

Polymorphic modifications

Electrical conductivity

Impedance spectroscopy

ABSTRACT

The formation of solid solutions $\text{Bi}_4\text{V}_{2-x}\text{Cu}_x\text{Ti}_{x/2}\text{O}_{11-x}$ ($0.025 \leq x \leq 0.5$) known as BICUTIVOX, synthesized by three different methods (a conventional solid-state synthesis, solid-state synthesis enhanced by mechanical activation, and through liquid precursors), has been studied. Based on crystal structure investigations carried out at different temperatures, ranges of stability and temperatures of phase transitions for different polymorphous modifications have been defined. The morphology and the local chemical composition of the ceramic samples obtained have been studied. Thermal expansion coefficients have been measured. The electrical conductivity of ceramic samples has been investigated in a wide range of temperatures and partial oxygen pressures.

© 2011 Elsevier B.V. All rights reserved.

1. Introduction

Solid solutions of $\text{Bi}_4\text{V}_{2-x}\text{ME}_x\text{O}_{11-x}$ based on the $\text{Bi}_4\text{V}_2\text{O}_{11}$ bismuth vanadate with vanadium partly substituted by metal (ME) cations (BIMEVOX family) attract a lot of attention due to their high oxygen-ion conductivity at moderate temperatures. In general, the crystal structure of the parent bismuth vanadate can be described as alternate fluorite-like $(\text{Bi}_2\text{O}_2)^{2+}$ and perovskite-like $(\text{VO}_3\Box_{0.5})^{2-}$ layers, where \Box refers to structural vacancies in the anionic sublattice, which allow oxygen ions to move through the crystal. The $\text{Bi}_4\text{V}_2\text{O}_{11}$ compound exists in four polymorphic modifications: α , β , γ and γ' . Phase transitions temperatures are about 450 °C ($\alpha \rightarrow \beta$), 570 °C ($\beta \rightarrow \gamma$) and 870 °C ($\gamma \rightarrow \gamma'$). For the majority of solid solutions in the BIMEVOX family the highest electrical conductivity is observed for the high-temperature γ -modification. The γ -type structural polymorph can be stabilized down to room temperature by various ME elements independently of the electronic configuration, the formal valence and in most cases the preferential O coordination of the dopant, for example Nb^{V} , Ta^{V} , Sb^{V} , Cu^{II} , Ni^{II} , Fe^{III} , Mn^{IV} , Ti^{IV} , Co^{II} , Zn^{II} , Ca^{II} , Zr^{IV} , Al^{III} , In^{III} etc. [1–4]. It has been shown in several publications [5–10] that the γ -modification can be stabilized at room temperature also if vanadium is substituted by two cations with different valence. For

instance, simultaneous substitution of vanadium by Cu(II) and Ti(IV) results in the formation of solid solutions with rather high electrical conductivity values [6]. Substitution of vanadium by Nb(V) and Cu(II) with 10% overall amount of dopants results in the formation of two $\text{Bi}_4\text{V}_{1.8}\text{Cu}_{0.2-x}\text{Nb}_x\text{O}_{10.7+3x/2}$ solid solutions: the first, with $0 < x < 0.05$, crystallizes in the tetragonal γ -modification and the second, with $0.1 < x < 0.15$, crystallizes in the β -modification [7]. An increase of the Nb content leads to an increase of the unit cell parameters and the concentration of oxygen vacancies in the structure and results in a higher electrical conductivity of $\text{Bi}_4\text{V}_{1.8}\text{Cu}_{0.15}\text{Nb}_{0.05}\text{O}_{10.625}$ in comparison with the $\text{Bi}_4\text{V}_{1.8}\text{Cu}_{0.2}\text{O}_{10.7}$ solid solution doped with copper solely. The same was observed for the $\text{Bi}_2\text{V}_{0.9}\text{Co}_y\text{Cu}_{0.1-y}\text{O}_{5.35}$ ($0 < y < 0.1$) solid solutions, the electrical conductivity of which in the low-temperature region increases gradually with increasing Co concentration [8] and the electrical conductivity of $\text{Bi}_4\text{V}_{1.8}\text{Cu}_{0.2-x}\text{Co}_x\text{O}_{11-\delta}$ is slightly improved compared with the $\text{Bi}_4\text{V}_{1.8}\text{Cu}_{0.2}\text{O}_{11-\delta}$ such as in the case of Ti^{4+} – Cu^{2+} double substitution [11]. Besides double substitution of V by Co^{2+} and Cu^{2+} in the limit of 10% stabilizes at room temperature tetragonal γ -polimorph [11]. Still there have been only a few papers on double substitutions and that is why the present paper seems to be topical.

For $\text{Bi}_4\text{V}_{2-x}\text{Cu}_x\text{Ti}_{x/2}\text{O}_{11-x}$ ($0.025 \leq x \leq 0.5$) solid solutions, which are the main subject of the present paper, several results are reported in the literature [9,12]. In Ref. [5] the $\text{Bi}_2\text{V}_{0.9}\text{Cu}_{(0.1-x)}\text{Ti}_x\text{O}_{5.35+x}$ ($0 \leq x \leq 0.1$) solid solution is described. Samples with dopant concentration equal to $x=0$, 0.025, 0.05 were described as the

* Corresponding author. Tel./fax: +7 343 2617411.

E-mail address: morphey_usu@mail.ru (M.V. Morozova).

high-temperature γ -modification. $\text{Bi}_2\text{V}_{0.9}\text{Cu}_{0.05}\text{Ti}_{0.05}\text{O}_{5.3}$ showed the highest conductivity at temperatures 500 °C and 600 °C. However, at low temperature (300 °C) the highest conductivity is displayed by the specimen without titanium – $\text{Bi}_2\text{V}_{0.9}\text{Cu}_{0.1}\text{O}_{5.35}$. The authors believe that this fact is due to the electronic contribution to the total conductivity; the value of the electronic contribution is higher for the solid solution with double substitution by copper and titanium in comparison with copper substitution only.

It has been shown in our previous work [12] that the $\text{Bi}_4\text{V}_{2-x}\text{Cu}_{x/2}\text{Ti}_{x/2}\text{O}_{11-x}$ ($x < 0.30$) solid solution can be formed by the simultaneous substitution of vanadium by copper and titanium in the crystal structure. We refined the ranges of stability of different polymorphic modifications. It has been shown that a small total concentration of dopants ($x = 0.05\text{--}0.15$) results in a distortion of the initial monoclinic $\text{Bi}_4\text{V}_2\text{O}_{11}$ structure. At $x = 0.20$ the compound has an orthorhombic unit cell (sp.gr. *Amam*). A higher content of dopants ($x = 0.25\text{--}0.30$) leads to the formation of the tetragonal γ -modification (sp. gr. *I4/mmm*).

In the present work we continue our earlier studies with a detailed crystal structural investigation, a study of phase transitions and a description of some physicochemical properties of the $\text{Bi}_4\text{V}_{2-x}\text{Cu}_{x/2}\text{Ti}_{x/2}\text{O}_{11-\delta}$ solid solutions.

2. Experimental

$\text{Bi}_4\text{V}_{2-x}\text{Cu}_{x/2}\text{Ti}_{x/2}\text{O}_{11-\delta}$ ($0.025 \leq x \leq 0.5$) solid solutions were synthesized using different techniques: a conventional solid-state synthesis, a solid-state synthesis enhanced by mechanical activation, a synthesis through liquid precursors. For the conventional solid-state synthesis stoichiometric mixtures of Bi_2O_3 (99.9%), CuO (99.9%), TiO_2 (99.9%) and V_2O_5 (99.9%) were crushed in ethanol and annealed in air in the temperature range 500–800 °C with a step of 30–50 °C. Samples were kept at each temperature for 8–20 h and cooled with a rate of 250 K/min after the final heating. Preliminary mechanical activation was performed using an AGO-2 planetary ball mill. A centrifugal acceleration of $g = 60$ and a maximum treatment time of 23 min were used. The synthesis through liquid precursors involved the preparation of bismuth and copper nitrate solutions of the required concentration. Vanadium oxide was dissolved either in hydrogen peroxide or in citric acid with a 1:3 mass ratio which led to the formation of vanadate citrate $2(\text{VO})\text{C}_6\text{H}_6\text{O}_7$. Titanium was added in the form of tetrabutyl- or tetraethoxy-titanium, $\text{C}_{16}\text{H}_{36}\text{O}_4\text{Ti}$ and $\text{C}_8\text{H}_{20}\text{O}_4\text{Ti}$, respectively. The prepared solutions were mixed and then heated, and evaporated at $T = 100\text{--}120$ °C to obtain residual powder. Final annealing was carried out at $T = 600$ °C and 700 °C for 6–8 h each stage. The phase compositions of the obtained powders were checked by X-ray powder diffraction (DRON-3 diffractometer, by “Bourestnik”, Russia, $\text{CuK}\alpha$ -radiation, pyrolytic graphite monochromator in the diffracted beam). Precise crystal structure investigations and high-temperature X-ray diffraction studies were performed using a D8 ADVANCE diffractometer by “Bruker”, Germany ($\text{CuK}\alpha$ -radiation, β -filter, PSD VANTEC1) equipped with high-temperature chamber HTK1200N (Anton Paar). The samples were heated in the range 303–1023 K at a rate of 0.5 K/s. Indexing of the diffraction patterns, and

refinement of the cell parameters and crystal structure were done using the TOPAS [13] and LMGP [14] software packages. Particle sizes were determined using a SALD-7101 Shimadzu particle-size analyzer. The morphology of the obtained powders and their chemical composition has been studied using a JEOL JSM6390 LA scanning electron microscope equipped with a JED-2300 energy dispersive X-ray detector. The elemental compositions were determined by inductively coupled plasma atomic emission spectroscopy (ICP-AES) using an iCAP 6500 Thermo Scientific spectrometer. Electrical conductivity measurements of ceramic samples were performed on Elins Z-2000 and Elins Z-350 M impedance spectrometers in the temperature range 200–800 °C and oxygen partial pressure range $0.21\text{--}10^{-4}$ bar. Thermal dilatometric analysis was carried out using a DIL 402 C Netzsch dilatometer equipped with a vacuum furnace in the temperature range 20–650 °C with a heating rate of 2 K/min. The samples for dilatometric measurements were prepared as rectangular briquettes 25 mm length and those for impedance spectroscopy investigations – in the form of circular briquettes about 10 mm thick and 2–5 mm length. In both cases ceramic samples were sintered afterwards at 800–830 °C for 10–12 h.

3. Results and discussion

3.1. Synthesis and characterization of $\text{Bi}_4\text{V}_{2-x}\text{Cu}_{x/2}\text{Ti}_{x/2}\text{O}_{11-\delta}$ ($0.025 \leq x \leq 0.5$) solid solutions

The application of different synthesis techniques affects the composition range of solid solutions $\text{Bi}_4\text{V}_{2-x}\text{Cu}_{x/2}\text{Ti}_{x/2}\text{O}_{11-\delta}$ based on different structural modifications. Ranges of stability for each solid solution obtained by the different synthesis techniques are compared in Table 1. From Table 1 one can see that the conventional solid-state synthesis with fast cooling after the final heating stabilizes the γ -modification of BICUTIVOX (sp. gr. *I4/mmm*) at room temperature for $x \geq 0.25$. At first X-ray powder diffraction patterns of solid solutions with $x = 0.025\text{--}0.15$ were indexed in a monoclinic unit cell (sp. gr. *C2/m*). However, a precise X-ray powder diffraction study revealed lower symmetry. A whole-pattern decomposition [15] shows that substitution of vanadium ($R_{\text{V}^{5+}} = 0.59$ Å) by small amounts of dopants with larger ionic radii ($R_{\text{Ti}^{4+}} = 0.64$ Å, $R_{\text{Cu}^{2+}} = 0.72$ Å) [16] results in a distortion of the α - $\text{Bi}_4\text{V}_2\text{O}_{11}$ monoclinic structure to a lower triclinic unit cell (sp. gr. *P-1*). Whole pattern decomposition results for $\text{Bi}_4\text{V}_{1.9}\text{Cu}_{0.05}\text{Ti}_{0.05}\text{O}_{11-\delta}$ calculated from (a) monoclinic (*C2/m*) and (d) triclinic (*P-1*) unit cells are given in Fig. 1. Observed and calculated patterns together with difference plot and Bragg positions are shown. The enlarged parts of the patterns (b–c, e–f) characteristic for triclinic distortion are presented for clearness. Cell parameters of the $\text{Bi}_4\text{V}_{2-x}\text{Cu}_{x/2}\text{Ti}_{x/2}\text{O}_{11-\delta}$ solid solution ($0.025 \leq x \leq 0.1$) are shown in Table 2.

Samples obtained by mechanochemical activation with subsequent annealing at 600 °C for 3 h display the γ -modification only for $x \geq 0.3$. Anisotropic broadening of diffraction peaks associated with crystallite size was observed for the $\text{Bi}_4\text{V}_{1.7}\text{Cu}_{0.15}\text{Ti}_{0.15}\text{O}_{11-\delta}$ sample from this series. The crystallite size estimated from the powder diffraction pattern by using the spherical harmonics function

Table 1
Stability ranges of the $\text{Bi}_4\text{V}_{2-x}\text{Cu}_{x/2}\text{Ti}_{x/2}\text{O}_{11-\delta}$ solid solutions ($0.025 \leq x \leq 0.5$) synthesized by different methods.

Synthesis method	Composition, x											
	0.025	0.05	0.1	0.15	0.2	0.25	0.3	0.35	0.4	0.45	0.5	
Conventional solid state synthesis	<i>P-1</i>				α (sp.gr. <i>C2/m</i>)		<i>P-1</i> and <i>Amam</i>		γ -Modification (sp.gr. <i>I4/mmm</i>)			
Using mechanical activation	α -Modification (sp.gr. <i>C2/m</i>)								γ -Modification (sp.gr. <i>I4/mmm</i>)			
Using liquid precursors	α -Modification (sp.gr. <i>C2/m</i>)								γ -Modification (sp.gr. <i>I4/mmm</i>)			

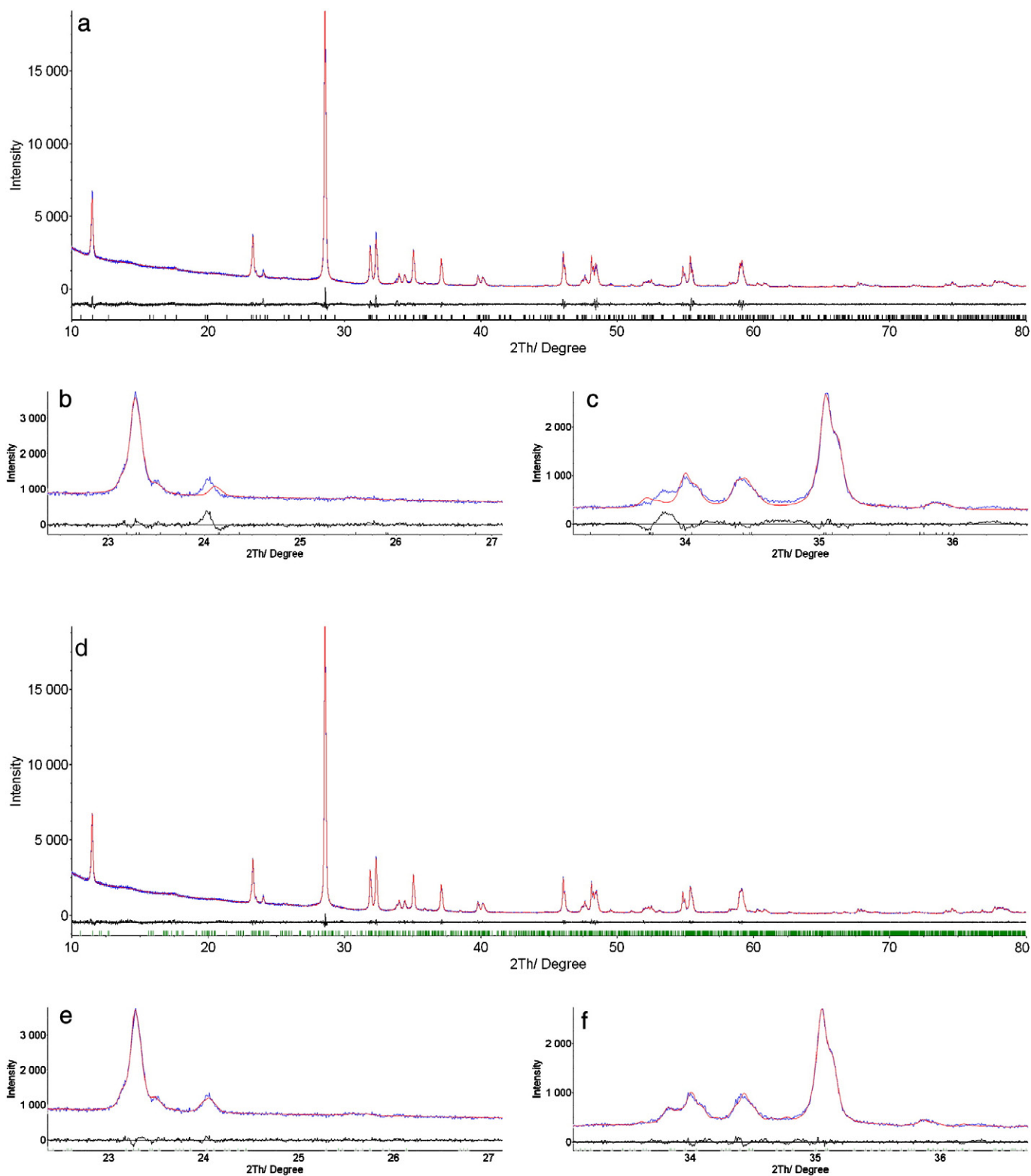


Fig. 1. X-ray experimental patterns (blue curve) and structure refinement results (red curve) for $\text{Bi}_4\text{V}_{1.9}\text{Cu}_{0.05}\text{Ti}_{0.05}\text{O}_{11-\delta}$ calculated from (a) monoclinic (C2/m) and (d) triclinic (P-1) unit cells together with difference plot and Bragg positions; b–c, e–f – the zoom on the triclinic distortion in both cases.

approach [17] was found to be about 160 nm with anisotropy equal to 25 nm. The visualization of the average crystallite shape and anisotropy according to calculation using the above mentioned approach is demonstrated in Fig. 2. Results of the $\text{Bi}_4\text{V}_{1.7}\text{Cu}_{0.15}\text{Ti}_{0.15}\text{O}_{10.7}$ crystal structure refinement are given in Table 3.

The synthesis using liquid precursors annealed at temperatures up to 700 °C allows one to obtain the γ -modification for compositions with $x=0.25, 0.3$. Samples with a higher concentration of dopants $x \geq 0.35$ contained, besides the γ -modification, a BiVO_4 impurity phase. The $\text{Bi}_4\text{V}_{1.65}\text{Cu}_{0.175}\text{Ti}_{0.175}\text{O}_{11-\delta}$ sample contains 1% of the

Table 2
Cell parameters of the $\text{Bi}_4\text{V}_{2-x}\text{Cu}_{x/2}\text{Ti}_{x/2}\text{O}_{11-\delta}$ solid solutions ($0.025 \leq x \leq 0.1$).

	Composition, x		
	0.025	0.05	0.1
a , Å	5.5887(2)	5.5861(2)	5.5794(3)
b , Å	15.2793(11)	15.3072(12)	15.3217(13)
c , Å	16.5979(14)	16.6283(13)	16.6265(17)
α , °	89.398(5)	89.323(4)	89.353(6)
β , °	89.867(8)	89.952(7)	90.069(7)
γ , °	89.473(2)	89.449(2)	89.429(3)
V , Å ³	1416.54(45)	1419.68(36)	1421.40(20)
Space group	$P-1$		
R_{wp}	4.18	4.27	4.19
$R_{\text{B}}\%$	0.401	0.396	0.235

BiVO_4 phase (a typical impurity for the BIMEVOX family). The crystal structure refinement of the considered solid solution revealed the presence of a few additional reflections with low intensity, which cannot be described by either the crystal structure model of the γ modification or that of BiVO_4 . Unindexed reflections are present at both small and wide angles; their intensity increases with increasing dopant concentration. We assume that these reflections come from another phase. Its content is estimated to be about 1% for $x=0.30$ and about 5% for $x=0.35$. The crystal structure of the third phase was described in a tetragonal basis (sp. gr. $I4/mmm$) with unit cell parameters: $a=3.913(1)$ Å, $c=15.581(2)$ Å and $a=3.9279(5)$ Å, $c=15.4756(15)$ Å, for $x=0.30$ and $x=0.35$, respectively. Fig. 3 shows the unit cell parameters of $\text{Bi}_4\text{V}_{2-x}\text{Cu}_{x/2}\text{Ti}_{x/2}\text{O}_{11-\delta}$ synthesized by the conventional solid-state method versus the dopant concentration x of the solid solution. The values of the cell parameters of the γ -modification (sp.gr. $I4/mmm$) are multiplied by $\sqrt{2}$ to unify coordinate systems.

The content of metal elements in the samples obtained was determined using inductively coupled plasma atomic emission spectroscopy (ICP-AES) and energy dispersive X-ray spectroscopy (EDS). Irrespective of the synthesis method used, an inhomogeneous distribution of titanium in the solid solutions was observed. Theoretical and experimental ratios of metal elements in the samples with dopant concentration $x=0.25, 0.30$ obtained by different synthesis procedures are given in Table 4. The metal ratios determined by ICP-AES show a slightly lower content of titanium in BICUTIVOX solid solutions compared with calculated values. The presence of micro-impurities with rich titanium content could be detected using scanning electron microscopy techniques and EDS. For instance, the fracture surface study of $\text{Bi}_4\text{V}_{2-x}\text{Cu}_{x/2}\text{Ti}_{x/2}\text{O}_{11-\delta}$ ($x=0.25, 0.30$) ceramic samples synthesized by the solid-state technique show that the $\text{Bi}_4\text{V}_{1.75}\text{Cu}_{0.125}\text{Ti}_{0.125}\text{O}_{11-\delta}$ sample is

Table 3
Atomic coordinates and isotropic thermal displacement parameters of $\text{Bi}_4\text{V}_{1.7}\text{Cu}_{0.15}\text{Ti}_{0.15}\text{O}_{10.7}$ obtained by solid-state reaction enhanced by mechanical activation, sp. gr. $I4/mmm$. $a=3.9313(5)$ Å, $c=15.4472(3)$ Å, $V=238.748(7)$ Å³.

Atom	Multiplicity	x/a	y/b	z/c	Occupancy	B_{iso}
Bi	4	0.0	0.0	0.1684 (1)	0.986 (11)	1.38 (10)
V/Ti	4	0.5	0.5	0.0012 (2)	0.458 (8)	0.93 (9)
Cu	4	0.5	0.5	0.0012 (2)	0.027 (7)	0.93 (9)
O1	4	0.0	0.5	0.25	0.41 (3)	1.02 (15)
O2	4	0.5	0.5	0.098 (3)	0.55 (3)	1.02 (15)
O3	8	0.5	0.0	0.036 (2)	0.38 (3)	1.02 (15)
O4	16	0.5	0.336(3)	-0.013 (4)	0.27 (3)	1.02 (15)

GOF = 2.30; $R_{\text{exp}} = 1.93\%$; $R_{\text{p}} = 5.54\%$; $R_{\text{wp}} = 6.65\%$; $R_{\text{B}} = 2.466\%$.

homogenous, while $\text{Bi}_4\text{V}_{1.7}\text{Cu}_{0.15}\text{Ti}_{0.15}\text{O}_{11-\delta}$ contains copper-doped bismuth vanadate with inclusions of vanadium-doped titanium oxide (Fig. 4). Impurities of titanium oxide (with average size ~ 1 μm) have been found in the samples obtained through liquid precursor synthesis at dopant concentration $x \geq 0.25$ (Fig. 5). Thus, even for the samples which, judging from X-ray powder diffraction, do not contain any impurities, the distribution of titanium is found to be inhomogeneous. In contrast to copper, which easily substitutes vanadium atoms in the crystal structure, titanium substitutes vanadium only partly, forming micro-impurities, the composition of which varies from vanadium-doped titanium oxide to the $\text{Bi}_4\text{V}_{2-x}\text{Ti}_x\text{O}_{11-\delta}$ solid solution.

Particle sizes vary for powders obtained by the different methods. Applying liquid precursor synthesis results in obtaining powders with particles of smaller average size (0.5–15 μm) than in the case of solid-state synthesis (3–30 μm) independently of the sample composition. Powders synthesized by the mechanochemical method have the widest particle size distribution (0.5–30 μm) but with the enhanced fraction of small particles of about 1–5 μm in diameter.

The occurrence and the temperature of phase transitions were determined for several solid solutions using in-situ high-temperature X-ray powder diffraction and dilatometry. For instance, the $\text{Bi}_4\text{V}_{1.9}\text{Cu}_{0.05}\text{Ti}_{0.05}\text{O}_{11-\delta}$ solid solution undergoes two first-order phase transitions: $P-1 \rightarrow Amam \rightarrow I4/mmm$. The change in the X-ray powder diffraction patterns during these phase-transitions is shown in Fig. 6. All phase transitions described are reversible and kinetically slow. It has been found that the phase transition temperatures strongly depend on the dopant concentration: increasing the dopant content leads to an increase of the temperature at which the $\alpha \leftrightarrow \beta$ transition occurs and to a decrease of the temperature of the $\beta \leftrightarrow \gamma$ phase transition, resulting in a narrowing of the stability range of the $Amam$ modification and a broadening of the stability range of the γ -modification (Table 5).

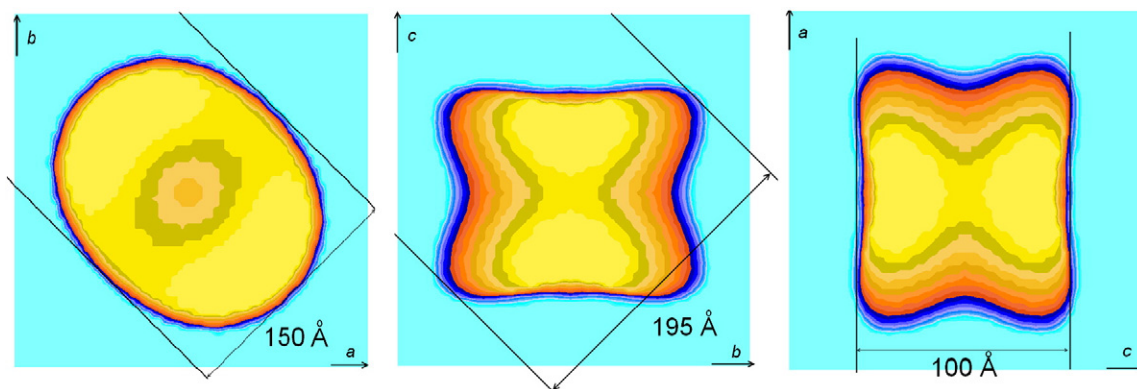


Fig. 2. Average crystallite shape: (a) xy -, (b) yz - and (c) zx -views according to the spherical harmonics function approach calculations.

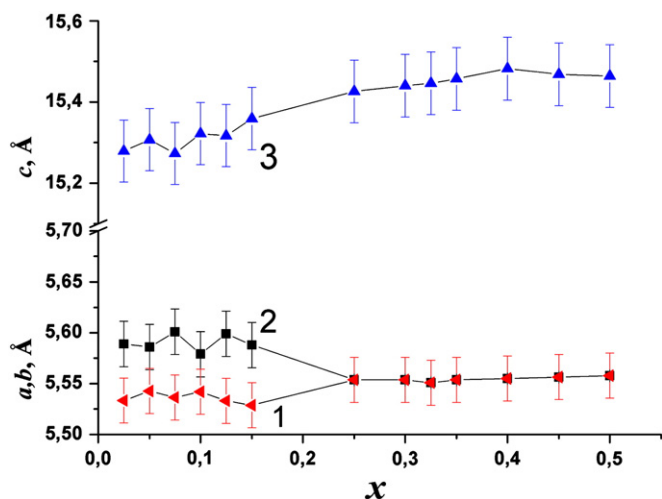


Fig. 3. Unit cell parameters ($a - 1$, $b - 2$, $c - 3$) vs. dopant concentration in $\text{Bi}_4\text{V}_{2-x}\text{Cu}_{x/2}\text{Ti}_{x/2}\text{O}_{11-\delta}$ solid solutions. Calculation error does not exceed 0.05% of magnitude.

Table 4

Metal ratios of BICUTIVOX samples.

x	Synthesis method	Bi:V:Cu:Ti		
		Theoretical value	EDS	ICP-AES
0.25	Solid-state	4.00:1.75:0.125:0.125	4.06 (7):1.71 (3):	4.00 (8):1.70 (5):
			0.15 (4):0.09 (5)	0.127 (5):0.034 (3)
0.3	Mechanical activation	4.00:1.70:0.150:0.150	4.1 (1):1.62 (5):	4.00 (8):1.58 (5):
			0.12 (7):0.12 (3)	0.119 (5):0.090 (3)
0.3	Mechanical activation	4.00:1.70:0.150:0.150	4.00 (7):1.68 (5):	4.00 (8):1.64 (5):
			0.255 (6):0.148 (5)	0.150 (5):0.095 (3)

The SEM (reflected electrons, WD = 10 mm; 20 kV) of ceramic samples used for dilatometry and impedance spectroscopy investigations are shown in Fig. 7. Here the contrast of the image is due to the

surface topography. Irrespective of synthesis method used the microstructure and porosity of the briquettes are alike. In general sample density and porosity may considerably impact TEC and impedance measurements but there is data that this influence is not critical for BIMEVOX samples [18,19]. The highest thermal expansion coefficients (TEC) were observed for $\gamma\text{-Bi}_4\text{V}_{2-x}\text{Cu}_{x/2}\text{Ti}_{x/2}\text{O}_{11-\delta}$ with content of dopants $x = 0.125\text{--}0.25$. It is worthy to mention that the obtained values are comparable with those for lanthanum-strontium cobaltites ($\sim 20 \times 10^{-6} \text{ K}^{-1}$), which are often proposed as a cathode material for a BIMEVOX solid electrolyte.

The thermal stability of different polymorphic modifications during heating–cooling cycles has been checked. Two samples with structures based on the α - and γ -modifications were annealed in air for 2 weeks at temperatures 450, 550, 650, 700, 750, 810 °C (heating) and in reverse order (cooling). Temperatures were chosen according to the possible phase transitions of the solid solutions. The phase composition of the slowly cooled samples was checked at each step by means of X-ray powder diffraction. After heating at 550 °C, $\alpha\text{-Bi}_4\text{V}_{1.95}\text{Cu}_{0.025}\text{Ti}_{0.025}\text{O}_{10.95}$ and $\gamma\text{-Bi}_4\text{V}_{1.7}\text{Cu}_{0.15}\text{Ti}_{0.15}\text{O}_{10.7}$ samples included, in addition to the main phase, two bismuth vanadates: BiVO_4 (~4%) and $\text{Bi}_{3.5}\text{V}_{1.2}\text{O}_{8.25}$ (~1% and ~6%, respectively). Annealing at 650 °C leads to the complete restoring of both initial solid solutions. For the $\alpha\text{-Bi}_4\text{V}_{1.95}\text{Cu}_{0.025}\text{Ti}_{0.025}\text{O}_{10.95}$ sample further heating reveals the $P-1 \rightarrow I4/mmm$ (γ -modification) phase transition at 810 °C, completely reversible after annealing at 750 °C. The data obtained coincide with results of the in-situ high-temperature X-ray powder diffraction study of α -BICUTIVOX. For the $\gamma\text{-Bi}_4\text{V}_{1.7}\text{Cu}_{0.15}\text{Ti}_{0.15}\text{O}_{10.7}$ sample two phase transitions have been observed: $I4/mmm \rightarrow P-1$ (550 °C) $\rightarrow I4/mmm$ (650 °C). Thus, even if the γ -modification of the BICUTIVOX solid solution can be stabilized at room temperature, it cannot be kept stable during a long-term heating–cooling cycle.

3.2. Electrical conductivity of $\text{Bi}_4\text{V}_{2-x}\text{Cu}_{x/2}\text{Ti}_{x/2}\text{O}_{11-\delta}$ ($0.025 \leq x \leq 0.5$) solid solutions

Irrespective of the synthesis method applied, the impedance plots of the investigated samples show a behavior typical for the oxygen-conducting BIMEVOX family (Fig. 8). Changing the total dopant

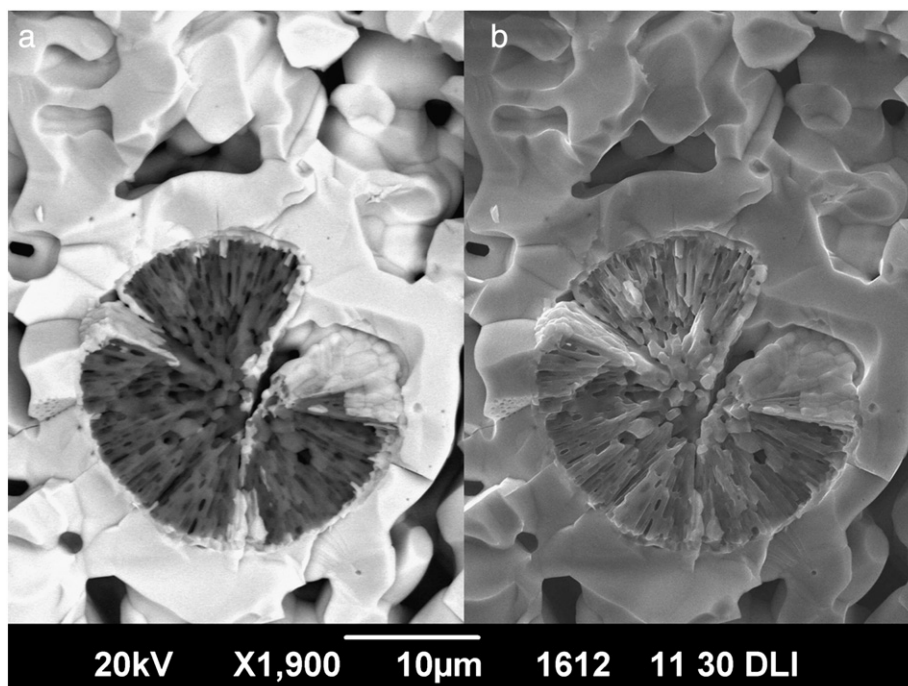


Fig. 4. Image of fractured surface of a $\text{Bi}_4\text{V}_{1.7}\text{Cu}_{0.15}\text{Ti}_{0.15}\text{O}_{11-\delta}$ ceramic sample. (a) Back-scattered electrons, (b) secondary electrons.

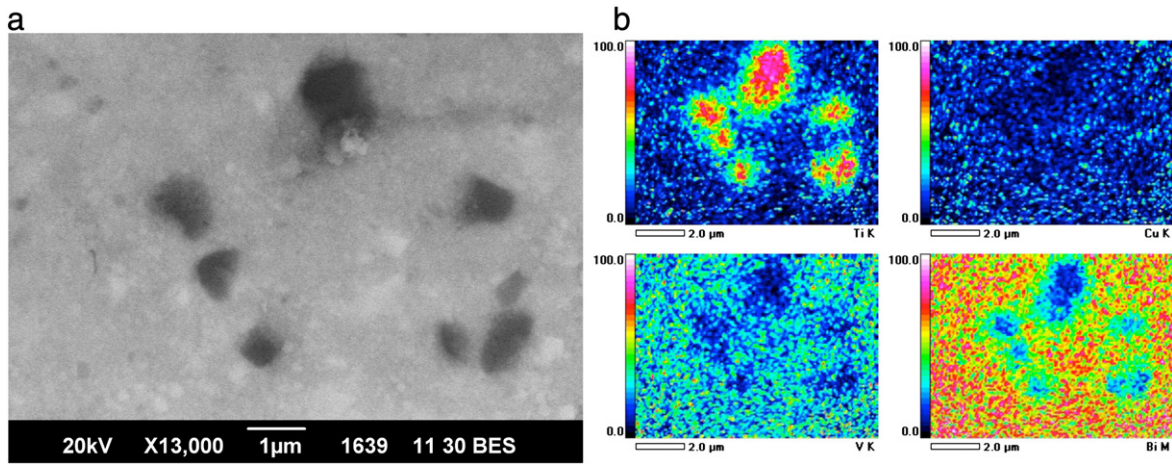


Fig. 5. (a) Backscattered electron image of polished surface of a $\text{Bi}_4\text{V}_{1.75}\text{Cu}_{0.125}\text{Ti}_{0.125}\text{O}_{11-\delta}$ ceramic sample. Inclusions of titanium oxide (dark gray grains) are observed in the $\text{Bi}_4\text{V}_{1.75}\text{Cu}_{0.25}\text{O}_{11-\delta}$ matrix; (b) X-ray maps for metal elements in the sample (Bi, V, Cu, Ti) taken from the same area, color scale refers to the concentration of the element given in atomic%.

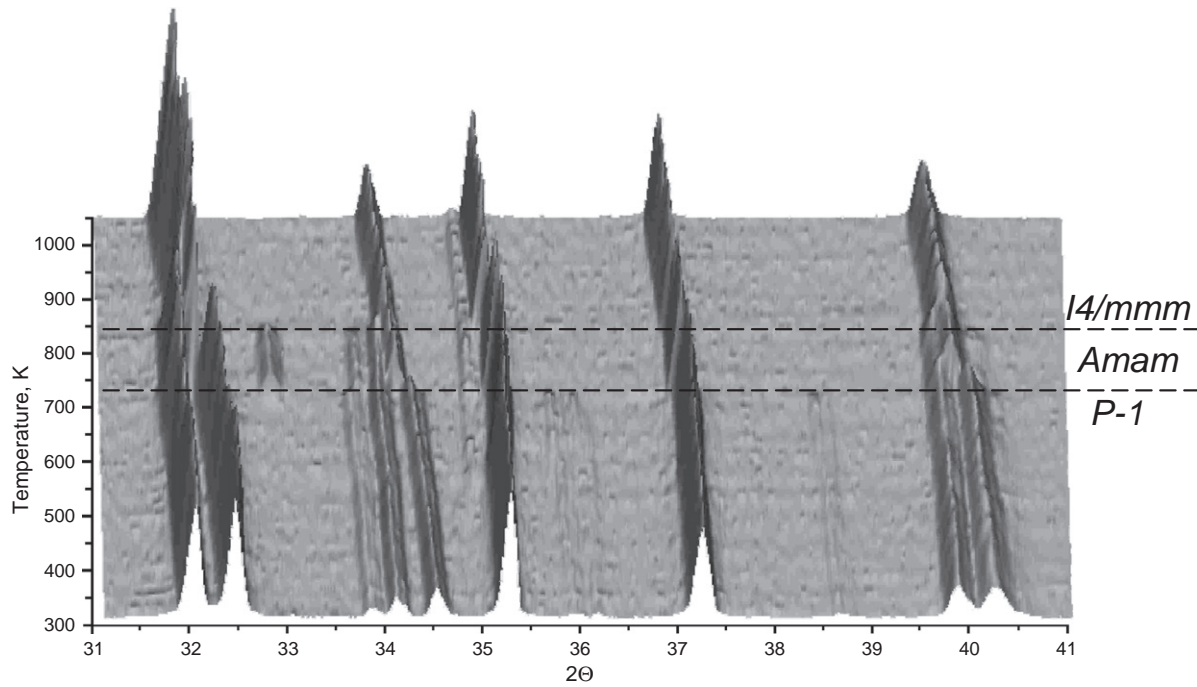


Fig. 6. Series of X-ray powder diffraction patterns of $\text{Bi}_4\text{V}_{1.9}\text{Cu}_{0.05}\text{Ti}_{0.05}\text{O}_{11-\delta}$ upon heating obtained for the 303–1023 K temperature range (heating rate 0.5°/s).

Table 5
Phase transition temperatures and TEC values for $\text{Bi}_4\text{V}_{2-x}\text{Cu}_{x/2}\text{Ti}_{x/2}\text{O}_{11-\delta}$.

Structure at room temperature	Composition, x	TEC $\alpha \times 10^6$, K^{-1} , $T > 600^\circ\text{C}$	Phase transition temperature, $^\circ\text{C}$			
			X-Ray data heating rate 0.5°/s		Dilatometry data, heating rate 2°/s	
			$\alpha \rightarrow \beta$	$\beta \rightarrow \gamma$	$\alpha \rightarrow \beta$	$\beta \rightarrow \gamma$
α (sp. gr. <i>P-1</i>)	0.025	22.3	360	520	445	560
	0.05		445	535	460	550
	0.075	21.4			460	525
	0.1	21.3	470	530	465	525
α (sp. gr. <i>C2/m</i>)	0.125	21.1			460	515
β (sp. gr. <i>Amam</i>)	0.2	20.4				470
γ (sp. gr. <i>I4/mmm</i>)	0.25	17.9				
	0.325					

concentration results in a shift of the plots and a change of their semi-circle diameters.

The temperature dependence of the electrical conductivity calculated from the impedance spectroscopy data of the $\text{Bi}_4\text{V}_{2-x}\text{Cu}_{x/2}\text{Ti}_{x/2}\text{O}_{11-\delta}$ ($x = 0.25, 0.30$) samples are shown in Fig. 9. The $\text{Bi}_4\text{V}_{1.7}\text{Cu}_{0.15}\text{Ti}_{0.15}\text{O}_{11-\delta}$ solid solution obtained by the conventional solid-state technique displays the highest conductivity. The slope of the plot $\lg \sigma$ vs. $1000/T$ slightly changes at $\sim 440^\circ\text{C}$ upon cooling due to the transition between the γ - and ordered γ' -modifications of $\text{Bi}_4\text{V}_{1.7}\text{Cu}_{0.15}\text{Ti}_{0.15}\text{O}_{11-\delta}$. In the remaining curves a sharp change of the slope at 500°C is observed; it appears due to a first-order phase transition from a higher (*I4/mmm*) to a lower (*P-1*) symmetry modification taking place upon cooling. Micro-impurities affect both the mechanical properties of the ceramics obtained (making them more fragile) and their electrical properties (decreasing the cumulative conductivity, see Fig. 10).

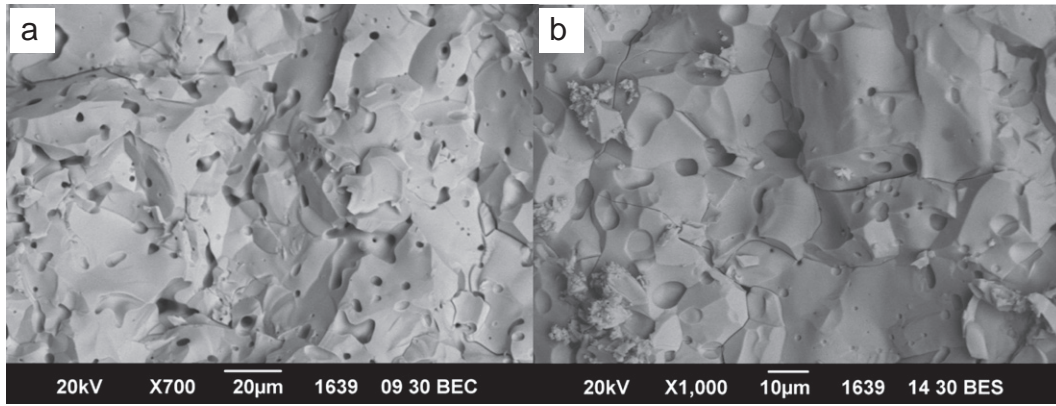


Fig. 7. SEM of BICUTIVOX sintered briquettes obtained of powder synthesized using liquid precursors (a) and conventional solid state method (b).

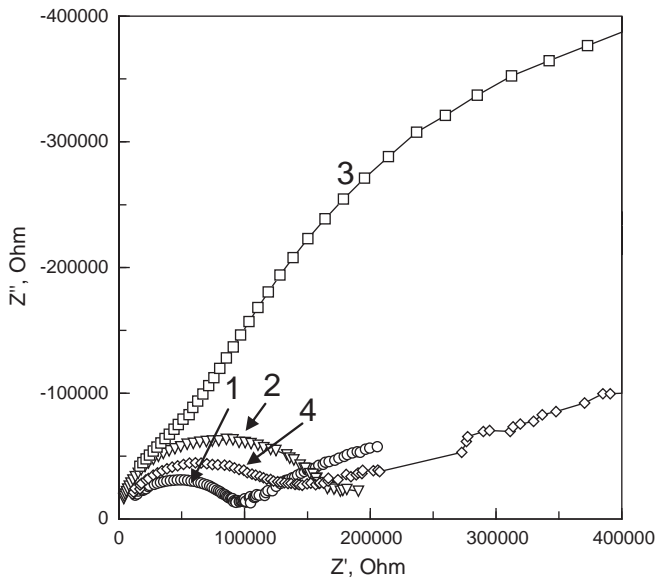


Fig. 8. Impedance plots of electrochemical cells with $\text{Bi}_4\text{V}_{2-x}\text{Cu}_{x/2}\text{Ti}_{x/2}\text{O}_{11-6}$ solid solutions as solid electrolyte and with Pt electrodes at 350 °C: 1 – $x=0.025$; 2 – $x=0.05$; 3 – $x=0.075$; 4 – $x=0.125$.

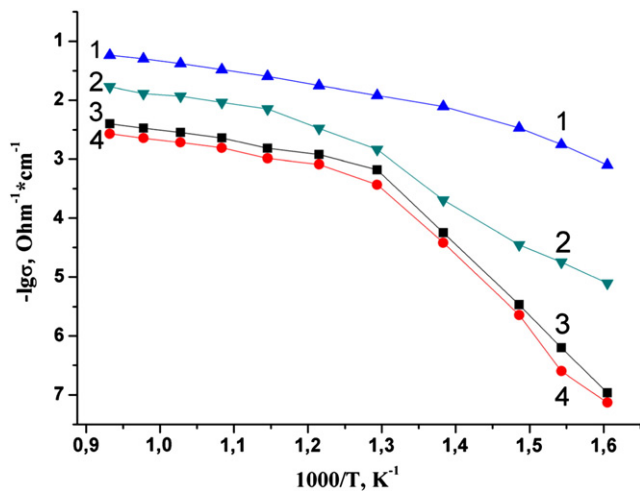


Fig. 9. Electrical conductivity vs. temperature for $\text{Bi}_4\text{V}_{2-x}\text{Cu}_{x/2}\text{Ti}_{x/2}\text{O}_{11-6}$, synthesized by various methods: 1 – solid-state method, $x=0.3$; 2 – mechanically activated, $x=0.3$; 3 – solid-state method, $x=0.25$; 4 – through liquid precursors, $x=0.25$.

The partial oxygen pressure dependences of the total conductivity calculated from impedance spectroscopy data for $\text{Bi}_4\text{V}_{1.65}\text{Cu}_{0.175}\text{Ti}_{0.175}\text{O}_{11-6}$ ceramics are shown in Fig. 11. For the studied partial pressures and temperature range (600–750 °C) the $\log \sigma = f(P_{\text{O}_2})$ curves were found to be parallel to the abscissa indicating a dominance of oxygen-ion conductivity in the investigated solid solutions. Similar results were obtained for BIFEVOX solid solutions [20]. Our results correlate with data obtained by Yaremchenko et al. [21] who proved that transfer numbers of oxygen ions in BICUVOX substituted by rare earth elements (La, Pr) are equal to 0.9–0.99 at 780–910 K.

4. Conclusions

Solid solutions $\text{Bi}_4\text{V}_{2-x}\text{Cu}_{x/2}\text{Ti}_{x/2}\text{O}_{11-6}$ ($0.025 \leq x \leq 0.5$) were synthesized using three different methods: a conventional solid-state synthesis, a solid-state synthesis enhanced by mechanical milling, and a synthesis through liquid precursors. A detailed crystal structure study at different temperatures allowed us to define and refine ranges of stability for different crystal structure modifications, and to estimate temperatures of phase transitions. The electrical conductivity of the ceramic samples was investigated within wide ranges of temperature and partial oxygen pressure. It is worthy to mention that in spite of rather high values of electrical conductivity ($2.5 \cdot 10^{-2} \text{ } \Omega^{-1} \cdot \text{cm}^{-1}$ at 750 °C) the synthesis and the practical usage

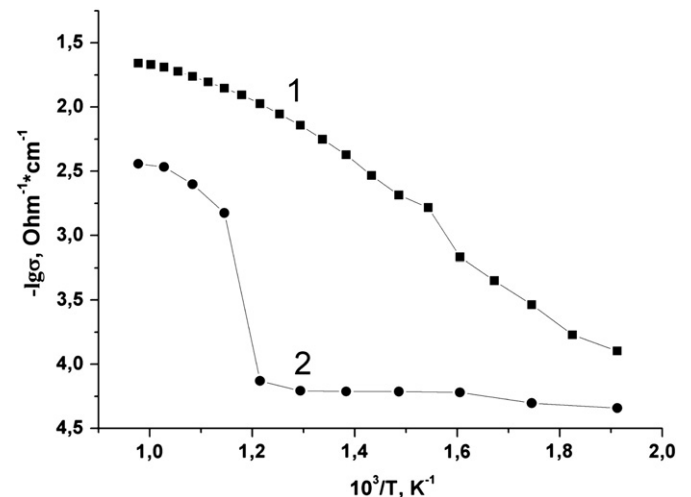


Fig. 10. Electrical conductivity of a single-phase $\text{Bi}_4\text{V}_{1.7}\text{Cu}_{0.15}\text{Ti}_{0.15}\text{O}_{11-6}$ sample (1) and one containing TiO_2 impurities (2).

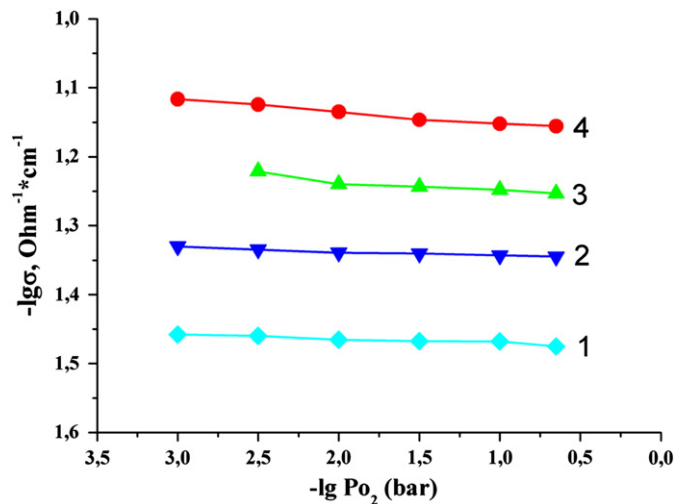


Fig. 11. Electrical conductivity of $\text{Bi}_4\text{V}_{1.65}\text{Cu}_{0.175}\text{Ti}_{0.175}\text{O}_{11-\delta}$ vs. partial oxygen pressures at several temperatures: 1 – 873 K; 2 – 923 K; 3 – 973 K; 4 – 1023 K.

of the investigated BITICUVOX solid solutions face some serious problems. These difficulties arise from both the appearance of non-controlled micro-impurities during the synthesis and the impossibility to stabilize the γ -modification of BITICUVOX in a wide temperature range.

Acknowledgments

This work was financially supported by the Russian Federal Agency for Education and Science within the “Scientific, research and educational personnel of innovative Russia, 2009–2013” federal program.

References

- [1] S. Lazure, Ch. Vernochet, R.N. Vannier, G. Nowogrocki, G. Mairesse, *Solid State Ionics* 90 (1996) 117.
- [2] S.J. Skinner, J.A. Kilner, *Mater. Today* (March 2003) 30.
- [3] V.V. Kharton, F.M.B. Marques, A. Atkinson, *Solid State Ionics* 174 (2004) 135.
- [4] N.M. Sammes, G.A. Tompsett, H. Nafe, F. Aldinger, *J. Eur. Ceram. Soc.* 19 (1999) 1801.
- [5] F. Abraham, Jc. Boivin, G. Mairesse, G. Nowogrocki, *Solid State Ionics* 40/41 (1990) 934.
- [6] M.H. Paydar, A.M. Hadian, G. Fafilek, *J. Eur. Ceram. Soc.* 21 (2001) 1821.
- [7] M. Alga, A. Ammar, B. Tanouti, A. Outzourhit, F. Mauvy, R. Decourt, *J. Solid State Chem.* 178 (2005) 2873.
- [8] F. Krok, I. Abrahams, M. Malis, W. Bogusz, J.A.G. Nelstrop, *Solid State Ionics* 3 (1997) 235.
- [9] M.H. Paydar, A.M. Hadian, G. Fafilek, *J. Mater. Sci.* 39 (2004) 1357.
- [10] R.N. Vannier, G. Mairesse, F. Abraham, G. Nowogrocki, *Solid State Ionics* 70–71 (1994) 248.
- [11] M. Alga, A. Ammar, R. Essalim, B. Tanouti, A. Outzourhit, F. Mauvy, R. Decourt, *Ionics* 11 (2005) 81–86.
- [12] Yu.V. Emelyanova, E.N. Tsygankova, S.A. Petrova, E.S. Buyanova, V.M. Zhukovskii, *Russ. J. Electrochem.* 43 (6) (2007) 737.
- [13] *DiffraC Plus: Topas Bruker AXS GmbH, Ostliche. Rheinbruckenstraße 50, D-76187, Karlsruhe, Germany, 2006.*
- [14] J. Laugier, B. Bochu, LMGP-Suite of Programs for the interpretation of X-ray Experiments. ENSP, Lab. Materiaux Genie Phys., Grenoble, 2003.
- [15] G.S. Pawley, *J. Appl. Cryst.* 14 (1981) 357.
- [16] R.D. Shannon, *Acta Cryst.* 32 (1976) 751.
- [17] M. Jarvinen, *J. Appl. Cryst.* 26 (1993) 527.
- [18] S.P. Simmner, D. Suarez-Sandoval, J.D. Mackenzie, B. Dunn, *J. Am. Ceram. Soc.* 80 (1997) 2563.
- [19] C.H. Hervoches, M.C. Steil, R. Muccillo, *Solid State Sci.* 6 (2004) 173.
- [20] M.V. Morozova, E.S. Buyanova, Ju.V. Emelyanova, V.M. Zhukovskiy, S.A. Petrova, *Solid State Ionics* 192 (2011) 153.
- [21] A.A. Yaremchenko, V.V. Kharton, E.N. Naumovich, F.M.B. Marques, *J. Electroceram.* 4 (1) (2000) 233.